IEEE Access
Multidisciplinary | Rapid Review | Open Access Journal

Received January 3, 2021, accepted January 12, 2021, date of publication January 18, 2021, date of current version February 1, 2021.

Digital Object Identifier 10.1109/ACCESS.2021.3051899

Heterogeneous Sensor Data Fusion for Human Falling Detection

DAOHUA PAN[1,2], HONGWEI LIU[1], AND DONGMING QU[3]

[1]School of Computer Science and Technology, Harbin Institute of Technology, Harbin 150001, China
[2]Department of Electronic and Information Engineering, Heilongjiang Vocational College for Nationalities, Harbin 150066, China
[3]Department of Financial Technology, China Construction Bank, Harbin 150001, China

Corresponding authors: Daohua Pan (pandaohua@ftcl.hit.edu.cn) and Hongwei Liu (liuhw@hit.edu.cn)

This work was supported by the National High Technology Research and Development Program of China (863 Program) "Cloud Computer Test and Evaluation System Development (2013AA01A215)."

ABSTRACT With the continuous improvement of human living standards, population aging has become a global development trend. At present, China has entered an aging society, the health and safety of the elderly have become the focus of social concern. Due to the aging of physiological structure and the decline of physical function, the probability and frequency of accidental falls in the elderly are very high. Under the above background, the purpose of this study is based on a heterogeneous sensor data fusion algorithm in an intelligent wearable sensor network. This article proposes a heterogeneous sensor data fusion algorithm based on wearable wireless body area network technology, and constructs a high-precision and stable wearable elderly activities of daily living (ADLs) and fall monitoring system. We first select the three-axis acceleration sensor, three-axis magnetic sensor, and three-axis angular velocity sensor to monitor the activities of the elderly. Then, we use Bluetooth to transmit the data collected by heterogeneous sensors to smartphones, and communicate with service centers and users through the mobile phone communication network, Family members interact to form a wireless city network based on wearable technology. Our proposed data fusion approach is based on the Kalman filter algorithm, which can reduce the system noise and improve the stability of the system. The experimental results demonstrate that the fall detection system proposed and implemented in this study can well detect accidental falls in the daily activities of the elderly, the sensitivity and specificity of the fall detection system are 98.7% and 98.5% respectively. The study in this article has a high research value and practical application significance in protecting the healthy life of the elderly.

INDEX TERMS Wearable sensor network, heterogeneous sensors, attitude measurement, data fusion.

I. INTRODUCTION

The rapid increase in the number of elderly people has brought great challenges to the medical system of the entire society. More and more wearable elderly health monitoring systems choose wearable wireless sensor body area networks for real-time and remote monitoring of the human body so that the user's family or doctor can grasp the patient's body condition in real-time [1]. At present, with the development of computer applications and the improvement of computer processing ability, the acquisition of human motion parameters becomes more scientific and reliable, and the research results are more and more valued by all walks of life. With the rapid development and maturity of microelectronic technology, the performance of various electronic components has been greatly improved, and the manufacturing process has also made considerable progress. The sensor is developing towards the direction of intelligence and miniaturization, which makes the motion recognition based on wearable sensors become the hot direction in the field of pattern recognition [2].

The wearable sensor network is a new technology that has developed rapidly in recent years. This is mainly due to the social development and improvement of living standards that have made people pay more and more attention to their own health. Medical treatment has also changed from passive treatment to active prevention and monitoring. The wearable sensor network embodies the concepts of mobile medical and

The associate editor coordinating the review of this manuscript and approving it for publication was Yanbo Chen.

telemedicine, and can provide people with personalized and ubiquitous medical care services. Life status monitoring and a series of research work provide a technical platform.

Falls in the elderly are a major public health problem in the world, as it often leads to disabling fractures. The accidental fall of the elderly has always been an important issue in social health care. According to statistics, nearly 30% of the world's elderly people over the age of 65 will fall accidentally every year. With the aggravation of the aging population in China, more and more attention has been paid to the accidental injury of the elderly due to falls. With the development of medical technology, a kind of health management (health card) service for the elderly or people with mobility difficulties has emerged, which is designed to help them carry out their daily life smoothly. With the advancement of the aging society, the proportion of elderly and weak patients who are unable to move due to old age is increasing year by year, so the demand for the above services is growing.

In recent years, heterogeneous sensor data fusion is a challenging field. Two of the challenges are learning from missing data and finding shared representations of multimodal data to improve reasoning and prediction. Zhang proposed a deep modal encoder (DME) based on the deep learning technology, which is used for sensor data compression, missing data filling, and new modal prediction. The traditional method only captures the intra-pattern correlation, while DME can simultaneously mine the intra-pattern correlation of the initial layer and the deeply enhanced pattern correlation. In this way, the statistical structure of sensor data can be better used for data compression. By introducing a new objective function, DME has a significant ability to fill the missing data in the sensor data [3]. Valero proposed a real-time monitoring decision-making method of Bayesian nonparametric Dirichlet process (DP) based on multiple heterogeneous sensor data. Under different experimental conditions, the sensor signal is obtained from the UPM device, which is composed of micro tri-axial force, tri-axial vibration, and acoustic emission (AE) sensors installed near the tool. They use an adaptive nonparametric DP modeling technology to track the obvious nonlinear and non-Gaussian signal patterns in the sensor data obtained by experiments [4].

This research mainly focuses on the heterogeneous sensor data fusion algorithm in the intelligent wearable sensor network. The algorithm combines the carrier attitude estimation method and the filtering algorithm. The former is used for the calculation and representation of human motion attitude, and the latter is used to improve the accuracy of the algorithm.

II. WEARABLE WIRELESS SENSOR NETWORK SYSTEM

A. WEARABLE WIRELESS SENSOR NETWORK ARCHITECTURE

1) WEARABLE WIRELESS SENSOR NETWORK STRUCTURE

Due to the development and expansion of the concept of wearable computers, wearable sensor networks came into being [5]. It is composed of wireless sensor nodes with different functions and is mainly deployed on low-power mobile

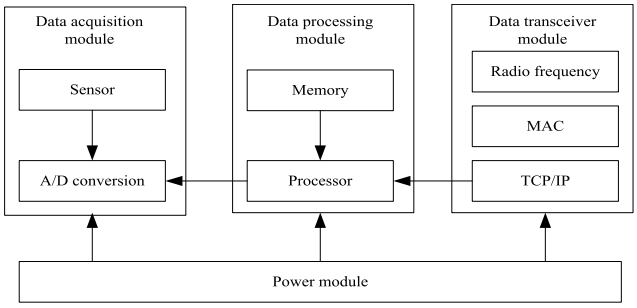

FIGURE 1. Node structure of a wearable wireless sensor network.

targets. Sensor nodes mainly include photoelectric sensors, temperature and humidity sensors, pressure sensors, etc. [6], [7]. The use of short-range wireless communication technology for communication between nodes is a sensor network that can intelligently sense information about the human body and its surrounding environment, and belongs to a new type of wireless sensor network [8], [9]. In the underlying data transmission stage, short-range wireless communication technologies such as Bluetooth, ZigBee, and Wi-Fi are mainly used to build a new wireless human body area network (WBAN), which is wireless, self-organizing, highly flexible, and even hidden. In this network, the sensor nodes mainly monitor the user's various movement status information in real-time, extract the characteristics of the collected data, merge the data, and use the wireless communication protocol to send the fusion result to the wireless communication module, and then, the received data send to the terminal device for processing. The biggest difference between wearable wireless sensor networks and wearable computers is that sensor networks can effectively complete decentralized control [10], [11].

2) SENSOR NODE STRUCTURE

Sensor networks belong to task-based networks, which are designed and deployed with different architectures according to different application backgrounds, especially with pertinence [12]. The general sensor node structure is shown in Figure 1.

Among them, the data acquisition module is composed of multiple wireless sensors with different functions and digital to analog conversion components, which are responsible for information acquisition and data conversion of the monitored area or object. The data processing module includes processor and memory, whose main task is to control the operation instructions of all sensor nodes, The data collected by itself or transmitted by other nodes are stored and processed. The main task of the data transceiver module is to transmit radio frequency signals, communicate with other sensor nodes wirelessly, and exchange control information and data collected by sensor nodes with each other. The power module is responsible for providing the energy required for normal operation of the wireless sensor nodes, Generally, micro-batteries are selected for power supply [13], [14].

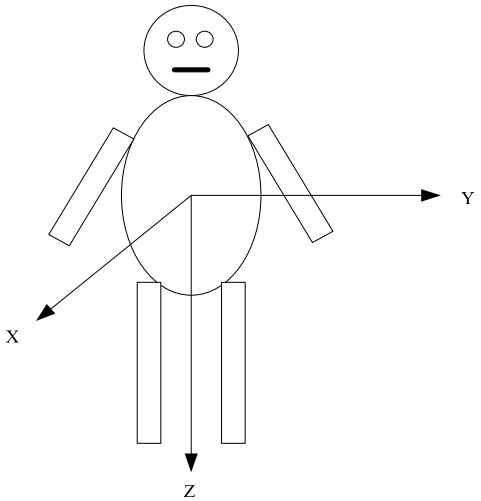

FIGURE 2. Three-dimensional human coordinate system.

B. DEFINITION AND TRANSFORMATION OF 3D COORDINATE SYSTEM

The posture of the human body is the azimuth relationship between the human body coordinate system and the geographical coordinate system, so this study involves two coordinate systems: the human body coordinate system and the geographical coordinate system [18].

For the inertial MEMS sensor, the human body coordinate system is the most basic coordinate system, because the inertial MEMS sensor is fixed on the human body and moves with the movement of the human body, so the sensor coordinate system and the human body coordinate system remain coincident [19], [20]. The three-dimensional human body coordinate system is shown in Figure 2. Its origin coincides with the center of mass of the human body. The x-axis points forward to the front of the human body, the y-axis points to the side of the human body to the right, and the z-axis vertically coincides with the gravity direction. The three axes are perpendicular to each other, and the arrow direction is positive, forming the right-hand coordinate system.

The geographic coordinate system is the local horizontal coordinate system, also known as the NED coordinate system or the inertial rectangular coordinate system, which is also represented by three mutually perpendicular vector axes that satisfy the right-hand orthogonal rule. Its origin coincides with the origin of the human body coordinate system. The N axis points to the north of the earth along the local meridian, the E axis points to the east of the earth along the local latitude, and the D axis coincides with the direction of gravity and points to the center of the earth [21].

Because the posture of the human body is expressed by the orientation relationship between the human coordinate system and the geographic coordinate system, it involves the conversion between the two coordinate systems. In the mathematical method, the conversion from one rectangular coordinate system to another rectangular coordinate system requires two operations of rotation and translation, but because translation does not change the direction of the coordinate system, only the coordinate rotation is considered here [22], [23]. The angular relationship between two spatial coordinate systems can be expressed by a matrix, namely the direction cosine matrix.

A three-dimensional rectangular coordinate system $OX_1Y_1Z_1$ is provided, and the unit vectors on its three axes are i_1, j_1, k_1, respectively. Any vector L can be represented by its components on three axes:

$$L = L_{X1}i_1 + L_{Y1}j_1 + L_{Z1}k_1 \tag{1}$$

Here, the component L_{X1}, L_{Y1}, L_{Z1} is the projection of the vector L on the three axes $X_1Y_1Z_1$, $|L|$ in the formula (2) is the modulus of the vector L, and θ^L_{X1}, θ^L_{Y1} and θ^L_{Z1} are the angles between the vector L and the three axes of the coordinate system $OX_1Y_1Z_1$ respectively [24], [25].

$$\begin{aligned} L_{X1} &= |L|\cos\theta^L_{X1} \\ L_{Y1} &= |L|\cos\theta^L_{Y1} \\ L_{Z1} &= |L|\cos\theta^L_{Z1} \end{aligned} \tag{2}$$

Obviously, when $\cos\theta^L_{X1}$, $\cos\theta^L_{Y1}$, and $\cos\theta^L_{Z1}$ are determined, the direction of the vector L relative to the coordinate system $OX_1Y_1Z_1$ is also determined, so $\cos\theta^L_{X1}$, $\cos\theta^L_{Y1}$, and $\cos\theta^L_{Z1}$ are called the direction cosine of the vector L in the coordinate system $OX_1Y_1Z_1$.

Now suppose there is another three-dimensional rectangular coordinate system $OX_2Y_2Z_2$, where the direction cosine of the X2 axis in three directions relative to the $OX_1Y_1Z_1$ coordinate system are $\cos\theta^{X2}_{X1}$, $\cos\theta^{X2}_{Y1}$, and $\cos\theta^{X2}_{Z1}$; the Y2 axis in three directions relative to the $OX_1Y_1Z_1$ coordinate system are $\cos\theta^{Y2}_{X1}$, $\cos\theta^{Y2}_{Y1}$,and $\cos\theta^{Y2}_{Z1}$; the Z2 axis in the three directions of the$OX_1Y_1Z_1$ coordinate system are $\cos\theta^{X2}_{Z1}$, $\cos\theta^{Z2}_{Y1}$, and $\cos\theta^{Z2}_{Z1}$; then there is a directional cosine matrix:

$$C_1^2 = \begin{bmatrix} \cos\theta^{X2}_{X1} & \cos\theta^{X2}_{Y1} & \cos\theta^{X2}_{Z1} \\ \cos\theta^{Y2}_{X1} & \cos\theta^{Y2}_{Y1} & \cos\theta^{Y2}_{Z1} \\ \cos\theta^{X2}_{Z1} & \cos\theta^{Z2}_{Y1} & \cos\theta^{Z2}_{Z1} \end{bmatrix} \tag{3}$$

$$L_2 = C_1^2 L_1 \tag{4}$$

L1 and L2 in formula (4) represent the column vectors of the coordinates of vector L in $OX_1Y_1Z_1$ and $OX_2Y_2Z_2$, respectively:

$$L_1 = \begin{bmatrix} L_{X1} & L_{Y1} & L_{Z1} \end{bmatrix}^T \tag{5}$$

$$L_2 = \begin{bmatrix} L_{X2} & L_{Y2} & L_{Z2} \end{bmatrix}^T \tag{6}$$

Since the nine elements in C_1^2 are the direction cosine between the coordinate axes of the two coordinate systems, it reflects the angular position relationship between the two coordinate systems, so the matrix C_1^2 links the two sets of coordinates of the same vector.

C. MATHEMATICAL MODEL OF DATA FUSION ALGORITHM

1) SAMPLING DATA MODEL

Because the measurement data of the sensor is not accurate enough, a single sensor is not enough to meet our accuracy

requirements for human activity measurement. In order to obtain satisfactory and accurate data, wireless sensor networks usually monitor the same target through multiple sensors of the same type, integrate the results of multiple sensors, merge relevant information, and perform overall calculations to get closer to the final result. Therefore, data fusion is based on sampling data from multiple sensors.

Suppose that at time t there are n sensors measuring the relevant parameters simultaneously in different directions. The sensor sequence can be expressed as $S(t) = \{S_1(t), S_2(t), \ldots, S_n(t)\}$, then:

$$s_1(t) = X + \eta_i(t), \quad i = 1, 2, \ldots n \tag{7}$$

In formula (7), $s_1(t)$ is the measured value of the sensor $S_1(t)$ at time t, X is the true value, $\eta_i(t)$ is the noise of the sensor at time t, and the prior knowledge $E[\eta_i(t)]$ and $D[\eta_i(t)]$ are unknown.

Record the sampled data from t_1 to t_m, the sampled data matrix is as follows:

$$D = \begin{Bmatrix} s_1(t_1) & s_1(t_1) & \cdots & s_1(t_1) \\ s_1(t_1) & s_1(t_1) & \cdots & s_1(t_1) \\ \vdots & \vdots & \ddots & \vdots \\ s_1(t_1) & s_1(t_1) & \cdots & s_1(t_1) \end{Bmatrix} \tag{8}$$

Each element in the matrix D represents the measured value of the sensor i at time t. The columns in the matrix represent the measured values of the sensor sequence at the same time. The rows in the matrix represent the sequence of sampled values of the same sensor over time. This form of sampling data is convenient for observation and comparison, and the data records are clear, which is convenient for taking values and is conducive to calculation. It is the most used data sampling model and expression in data fusion algorithms.

2) FUSION FUNCTION

The data measured by the sensor will be more or less affected by noise, so the measured data are different, and the impact of noise varies, these factors will make the difference between the data. In order to measure the size of the difference between the data, the absolute difference is used to quantify the "difference". The absolute distance is dis_{ij}:

$$dis_{ij} \left| s_i - s_j \right| \tag{9}$$

The definition of the absolute distance dis_{ij} is to measure the difference between the two data. It can be intuitively understood as the distance between the two values on the number axis. The distance is a non-negative concept, so it is expressed as an absolute value. The concept of absolute distance simply represents the difference between two numbers, but it plays an important role in the concept of fusion and is also the basis of fusion.

For the data in the sampling sequence D, if there is data that deviates from the overall trend and range of other data, then it can be considered that it is affected by a lot of noise, the deviation from the real value X is large. It can be considered that the proportion of this data occupied in the fusion process is smaller than other data, and its effect is lower. In order to measure the role of data in the fusion process, the concept of the fusion degree function is introduced. The fusion function can be expressed as follows:

$$c_{ij} = \exp\left\{R \bullet dis_{ij}\right\} \tag{10}$$

where R is a negative constant, and the fusion degree function describes the fusion degree of value s_i relative to value s_j. When the absolute distance between the two is large, it means that the fusion degree of the value s_i relative to the value s_j is small, and the fusion degree is low. The fusion degree function maps the absolute distance into the interval [0,1] and is a decreasing function, which meets the concept and requirements of the fusion degree.

3) FUSION DEGREE MATRIX

The fusion function is considered to be the relative degree of fusion between the two data. However, the degree of fusion of data should be compared with the entire sampling sequence D during the entire fusion process in order to describe its characteristics more objectively and accurately. To this end, the fusion degree matrix is introduced to facilitate overall calculation and analysis. The fusion matrix can be expressed as follows:

$$C = \begin{Bmatrix} 1 & c_{12} & \cdots & c_{1m} \\ c_{21} & 1 & \cdots & c_{2m} \\ \vdots & \vdots & \ddots & \vdots \\ c_{m1} & c_{m2} & \cdots & 1 \end{Bmatrix} \tag{11}$$

The element c_{ij} in the matrix represents the degree of fusion of the data s_i with respect to the data s_j in the sequence D. The diagonal elements of the fusion degree matrix are all 1, this is because the fusion degree of a data relative to itself does not make sense. It can be considered that its fusion degree with itself is 1. Therefore, in order not to let the data itself affect the estimation of the total fusion degree, in the data fusion algorithm, the row or column of the fusion degree matrix can be omitted by 1 to calculate other elements.

The multi-sensor data fusion algorithm is based on the fusion degree matrix and performs relevant calculations on the elements in the matrix to obtain the final fusion result. The fusion degree matrix is the cornerstone of the data fusion algorithm and has a very important role and significance.

4) FUSION RESULT EXPRESSION

For the sampled data sequence D, each data should be considered to have a certain degree of influence on the final fusion result. However, the magnitude of the influence is different depending on the deviation of each data from the overall trend of sequence D. Therefore, the weight coefficient is used to quantify the influence degree of each data on the final fusion result. The calculation of the weight coefficient has different calculation methods in different algorithms. But the weight coefficient has very important rules and characteristics. q_i represents the weighting coefficient of the data s_i.

Then there are:

$$q_1 + q_2 + \ldots + q_n = 1 \tag{12}$$

For extreme data, it is not excluded that the value of 11 is 1 or 0. However, the sum of the weight coefficients is q_i, and the weight coefficients are all non-negative and less than or equal to 1. The weight coefficient can be regarded as the output result of the fusion algorithm in a certain sense. When the calculation of the weight coefficient is completed, it means that the fusion result is determined. Therefore, the weighting factor can be regarded as the "final result". The final expression of the fusion result is as follows:

$$results = q_1 \times s_1 + q_2 \times s_2 + \ldots + q_n \times s_n \tag{13}$$

The fusion result is the product of each element in the sampling sequence and each weighting coefficient and then summation. It is not difficult to understand why the weight coefficient is actually the output of the algorithm, and it is also the "final result".

D. GENERAL SENSOR DATA FUSION ALGORITHM

The heterogeneous sensor data fusion algorithm is to synthesize the processed heterogeneous sensor information to form a way of expressing the characteristics of the external environment or the measured object. A single sensor can only get some information about the measured object, and after the fusion of the heterogeneous sensor information, it can accurately reflect the characteristics of the objective environment or object.

Because the MEMS sensor is susceptible to the edge of noise interference, Therefore, it is very necessary to filter the noise from the collected data information. Researchers in different fields have proposed different filtering methods according to their specific purposes. For example, Y. Chen *et al.* proposed a robust weighted least absolute value state estimation approach with optimal transformations (WLAV-OT) in 2015 and has been preliminarily tested with promising results [26]. They also proposed a robust state estimator based on maximum exponential absolute value (MEAV) in 2017, and make simulation tests based on the IEEE benchmark systems and two real grids of China to demonstrate the proposed MEAV estimator is very robust with high efficiency [27]. Y. Chen *et al.* also proposed a robust state estimation (SE) method based on second-order conic programming(SOCP) for the integrated electricity-heat system(IEHS) in 2020 [28].

Several filters such as Complementary filter, low pass filter, Kalman filter, Extended Kalman filter are used for sensor fusion in the last few decades. The complementary filter uses a relatively easy algorithm, which is easy to implement for it only requires less computation, it preferred for embedded systems. Using high pass filter and low pass filter remove accelerometer spike and Gyroscopic drift relatively. Kalman filter is an iterative filter, which is efficient but high computational complexity [29]. The advantage of Kalman filter is that it has very low memory. It works by correlating between current states and predicted states.

Kalman filter is an ideal filter for getting precise value. It is well known for its high accuracy. It is an ideal filter for getting precise value. Tariqul Islam *et al.* made an experiment compared complementary and Kalman filters, the result shows that after introducing the Kalman filter the curve is stable and the value is much more precise. Kalman filter is a more complex and considerate algorithm [30]. The Kalman filter algorithm can be used to optimize the estimated attitude angle during system implementation. The robustness and computational efficiency of the Kalman filter are tested in [31]. The working principle of the Kalman filter is mainly the following five formulas.

$$\hat{I}_t^- = F\hat{I}_t^- + Au_t \tag{14}$$

Among them: $\hat{I}_t^-$ is the prediction result inferred based on the state at the previous moment; F is the state transition matrix, and A indicates how to infer the state at the current moment from the previous moment; u_t indicates how the control variable acts on the current state.

$$P_t^- = FP_{t-1}F^T + Au_t \tag{15}$$

Among them: P_t^- is the noise covariance matrix, and F^T is the noise covariance matrix of the prediction model itself.

$$K_t = P_t^- G^T (GP_t^- G^T + R)^{-1} \tag{16}$$

Among them; K_t is the Kalman measurement coefficient; G^T is the conversion relationship between the predicted value and the observed value; R is the measurement noise covariance matrix.

$$\hat{Y}_t^- = \hat{Y}_{t-1}^- + K_t(Z_t - HX_t^-) \tag{17}$$

Among them: Z_t is the measured value.

$$P_t = (I - K_t H)P_t^- \tag{18}$$

In the above formulas, (15) and (16) are state prediction equations; (16), (17), and (18) are state update equations. By analyzing the above relational expressions, it is possible to measure the influence of a part of the noise elimination on the measured value of the MEMS acceleration sensor, which can greatly increase the accuracy of the measurement, reduce the system noise, and improve the stability of the system.

III. WEARABLE SENSOR NETWORK DATA FUSION EXPERIMENT

A. EXPERIMENTAL DATA COLLECTION

The construction process of an elderly action database based on the wearable sensors can be divided into the following four modules: action data acquisition module, action data processing module, background storage module, foreground query module.

The data acquisition module includes the following parts: recording the basic information (date, name, gender, height, weight) of the elderly participating in the experiment, which

is convenient for later on-demand query; the data acquisition and preprocessing (original data, format conversion data) of the elderly is the data source of the elderly action database. Among them, the original data is collected by volunteers wearing the wearable sensor modules.

The data processing module is to cut the original long data (including multiple action segments) according to each complete action segment interval.

The backend storage module will use PostgreSQL to design the database. It includes three pieces of information: basic information of human movement, data information of human movement, and schematic diagram of human movement. PostgreSQL software is used to input basic information about human movement. The PostgreSQL software is used to input the basic format of the data table; the MATLAB software is used to write the program, and the corresponding pieces of information are inserted in batches according to the basic format of the data table.

B. SELECTION OF EXPERIMENTAL SENSORS

The principle and structure of the sensor are different, so the first problem to be solved when using the sensor for measurement is the selection of the sensor, that is, the correct sensor is selected according to the measurement purpose and the measurement object. After the sensor is determined, the corresponding measurement method is determined accordingly, so the accuracy of the final measurement result depends to a certain extent on the selection of the sensor.

1) SELECTION OF ACCELERATION SENSOR

Adxl345 is a kind of low-power triaxial acceleration sensor with high resolution, which can reach 13 bits. There are four kinds of ranges, namely $-2G \sim +2G$, $-4G \sim +4G$, $-8g \sim +8g$, $-16g \sim +16g$. The output is in the form of a 16-bit binary complement, which can be accessed by the IIC or SPI interface. Adxl345 is chosen because it is suitable for mobile devices. It can not only measure the static acceleration of gravity, but also the dynamic acceleration caused by motion, and it has a very high cost performance. Its resolution can reach 3.9mg/lsb.

2) SELECTION OF ANGULAR VELOCITY SENSOR

L3g4200d is a low-power three-axis digital output gyroscope with three optional full scales, namely $\pm$ 250dps, $\pm$ 500dps, $\pm$ 2500dps. It has 16-bit rate data output and can communicate with the outside world through the digital interface IIC or SPI. When FS $=$ 250dps, the sensitivity is 8.75mdps/digit, FS $=$ 500dps, the sensitivity is 17.50mdps/digit, FS $=$ 2500, the sensitivity is 70mdps / digit.

3) SELECTION OF MAGNETIC SENSOR

Hmc5883l is a weak magnetic sensor chip with a digital interface, which is widely used in low-cost compass and magnetic field measurement. It is composed of an hmc118x series magnetoresistance sensor with high resolution, an integrated circuit including amplifier, automatic demagnetization driver, deviation calibration, and a 12-bit analog-to-digital converter, which makes the compass accuracy within the range of 1 to 2 degrees. The size of hmc5883l is 3mm * 3mm * 0.9mm, with 16 pins, adopting lead-free surface packaging technology.

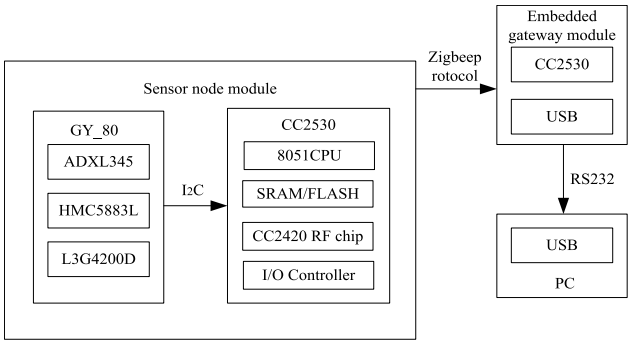

FIGURE 3. Structure diagram of wearable sensor network node platform.

C. STRUCTURE DESIGN OF EXPERIMENTAL PLATFORM

In the measurement system design, the MEMS sensor GY_80 contains three three-axis sensors. They are three-axis acceleration sensor, three-axis magnetic sensor, and three-axis angular velocity sensor. For the three-axis acceleration sensor, the ADXL345 sensor from Analog Devices is used in this study, which can provide an acceleration range of 2g-16g with a resolution of 3.9mg/LSB. The three-axis magnetic sensor uses Honeywell's HMC5883L three-axis digital compass, which can achieve a resolution of 5 milligauss in the measurement range of -8 gauss to 8 gauss. The three-axis angular velocity sensor uses ST's L3G4200D three-axis digital gyroscope with a range of 250dps to 2000dps. The data processing module uses CC2530, including 8051CPU, SRAM/FLASH, CC2420 radio frequency chip, and I/O controller, and other modules. Through the CC2430 RF chip module, based on the Zigbee protocol, the data is sent to the embedded gateway module, using the RS232 protocol of the USB interface to transfer the data to the PC. The hardware platform structure of the wearable sensor network node is shown in Figure 3.

IV. EXPERIMENTAL ANALYSIS OF HETEROGENEOUS SENSOR DATA FUSION ALGORITHM

A. NETWORK MODEL SIMULATION ANALYSIS

The experiment uses fuzzy neural network to collect data for training and evaluation and uses heterogeneous sensor data fusion algorithm for data fusion. The experimental parameter settings are shown in Table 1.

After evaluating the network convergence rate and network inference accuracy and other indicators, the performance of the data fusion algorithm is verified to be good, indicating that the data fusion algorithm is feasible. Compare the traditional T-S fuzzy neural network algorithm with the improved algorithm (as shown in Figure 4). The algorithm training convergence comparison chart illustrates the advantages of this algorithm.

TABLE 1. Related parameter setting table in simulation experiment.

Parameter	Value	Explanation
xite ()	0.001	Accuracy requirements
alfa ()	0.05	Learning rate
I	4	Enter the number of nodes
M	2	Number of implicit nodes, 2 membership functions
O	1	Number of output nodes
maxgen	1500	Maximum number of evolutions

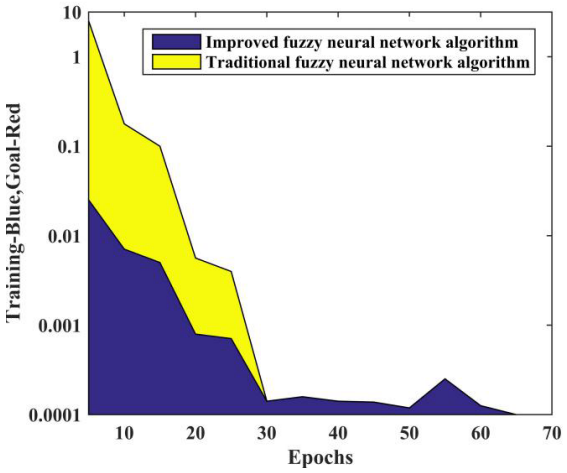

FIGURE 4. Convergence graph of traditional and improved fuzzy neural network algorithms.

It can be seen from Figure 4 that the traditional fuzzy neural network algorithm requires 65 steps to meet the error accuracy requirements. Since the improved algorithm avoids the slow and unstable network convergence caused by high-order partial derivatives, the network convergence speed is reduced from the previous 65 steps to 32 steps to complete the convergence, greatly reducing the network training time, indicating that the algorithm can improve network training Speed improves the real-time and stability of the network.

The heterogeneous sensor data fusion algorithm is used to compare the convergence speed between multiple nodes to illustrate the advantages of the data fusion algorithm proposed in this study in terms of energy saving of wireless sensor nodes.

As shown in Figure 5, in the time-consuming comparison experiment of multiple sensor nodes using heterogeneous sensor data fusion algorithm, when the frequency of the sensor node processor is different and the number of sensor nodes is different, the convergence speed of multiple sensor nodes is compared. With the same processor frequency, the smaller the number of sensor nodes, the longer the data fusion time; the same number of sensor nodes, as the processor frequency increases, the data fusion time decreases. When the processor frequency is greater than 2000hz, the convergence speed of the heterogeneous sensor data fusion algorithm is only related to the number of nodes. It can be concluded that the data fusion algorithm is effective.

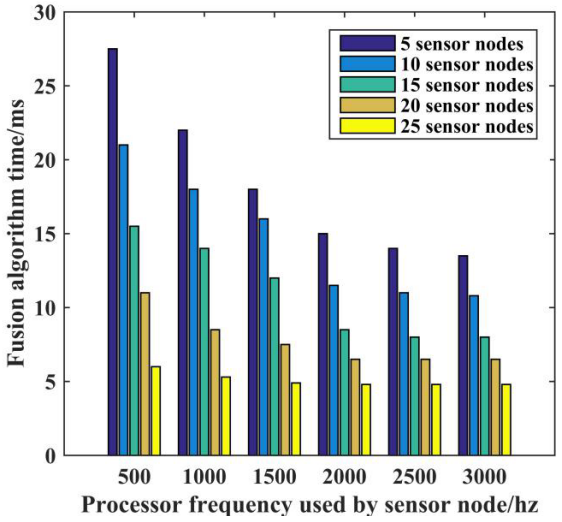

FIGURE 5. Time-consuming comparison of data fusion algorithms on multiple sensor nodes.

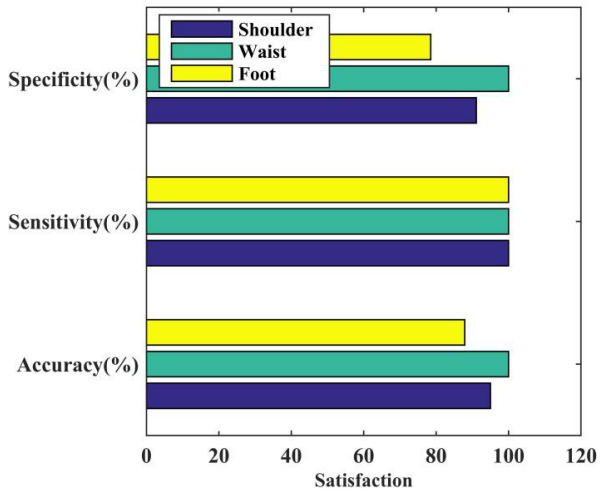

FIGURE 6. The accuracy, sensitivity and comfort of fall detection results for different body parts.

In the analysis of the result of misjudgment, it is agreed that the case of falling down but not sounding the alarm is a serious misjudgment, and the case that the alarm is sounded without falling is a general misjudgment. In the experiment, no matter which sensor module is placed in the three parts of the human body, the occurrence rate of serious misjudgment is 0, which proves that the fall detection system has good robustness; when the sensor module is placed in the shoulder and foot of the human body, the general misjudgment occurs respectively. According to the ratio of general misjudgment, the following conclusion can be drawn: when other conditions are the same, the system has good robustness, The sensor module is placed in the waist of the human body, and the accuracy of the data measured is the highest, followed by the shoulder, and finally the foot. The accuracy, sensitivity, and comfort of different parts of the body are shown in Figure 6.

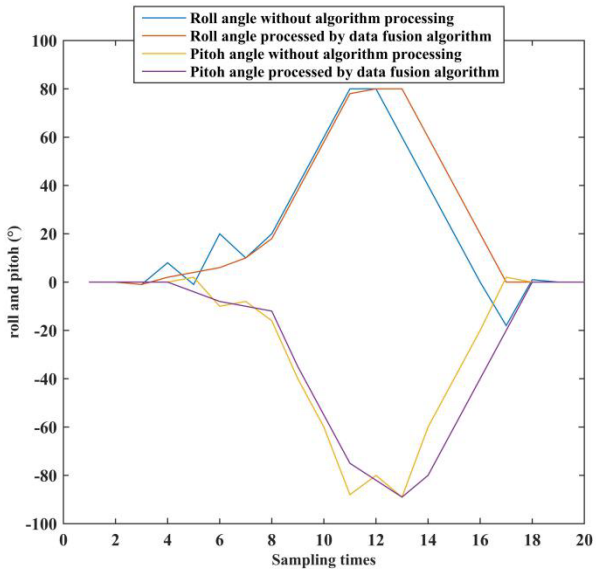

FIGURE 7. Comparison of roll and pitch angles which are processed by data fusion algorithm and without algorithm processing.

B. ANALYSIS OF ALGORITHM RESULTS

In order to prove the accuracy and effectiveness of the proposed data fusion algorithm, the posture data processed by the data fusion algorithm and the posture data not processed by the data fusion algorithm are compared and analyzed. The effect is shown in Figure 7.

As Figure 7 illustrates, the fluctuation of the curve is caused by the angle curve, which is not processed by the algorithm due to data errors, especially at the beginning and end of the experiment. The smoothness of the curve processed by the algorithm is good, and it is in good agreement with the unprocessed curve, indicating that the algorithm helps reducing errors and improving data accuracy.

The computational efficiency of the proposed data fusion algorithm is an important evaluation indicator. The computational efficiency of the Kalman filter algorithm can be estimated by the number of multiplications per cycle. One cycle can be divided into two parts: the predict part and the update part (the predict part subscript as P and the update part subscript as U). The number of multiplications M is computed using the standard formula, assuming that the components of the measurement are independent and taking advantage of the symmetric matrices i.e., only the upper triangular matrix has to be computed [32].

1. Predict Part: $M_P = \frac{3}{2}n^2(n+1)$

2. Update Part: $M_U = nm\left(\frac{3}{2}(n+m)+3\right)+\frac{2}{3}(m^3-m)$

2.1 Update Via Inverse: $M_{U,I} = nm\left(\frac{3}{2}n+\frac{7}{2}\right)+\frac{4}{3}(n^3-n)$

3. Data Compression: $M_D = m^3\left(\frac{7}{6}k+\frac{2}{3}\right) + m^2\left(\frac{7}{2}k+1\right)-m\frac{2}{3}(k+1)$

4. Estimate Compression: $M_E = (k+1)n\left(\frac{2}{3}(n^2-1)+n\right)$

Where n, m represent the number of rows and columns in the matrix, k is the maximum of m-dimensional data sets [32].

TABLE 2. Daily activity test results.

Testing scenarios	Number of experimental tests	Alarm times	Correct rate	False alarm rate
Walking straight	50	0	100%	0%
Walking turn	50	0	100%	0%
Stand to sit	50	0	100%	0%
Stand to squat	50	1	98%	2%
Walk upstairs	50	1	98%	2%
Walk downstairs	50	2	96%	4%

TABLE 3. Fall test results.

Testing scenarios	Experiments	Alarm times	Correct rate	False negatives	False alarm rate
Fall forward	50	48	96%	2	4%
Fall backward	50	49	98%	1	2%
Fall to the left	50	50	100%	0	0%
Fall to the right	50	50	100%	0	0%

The indicators of fall tests include false alarm rate and false-negative rate. Therefore, in the test, the experiment is divided into two groups, one is daily activities, that is, non-fall scene, to test the false alarm situation of the system; the other group is the fall scene to test the false alarm situation of the system. The daily activity scenarios include straight walking, walking and turning, standing to sit, standing to squat, walking upstairs, and walking downstairs. The test falls include falling forward, falling backward, falling to the left, and falling to the right. Each test object is divided into 5 groups. When preparing for the training data, each daily activity scene should last for 1 minute without interruption to ensure that the completed training sample data are collected. In addition, there is no limit on the time of the fall scene, but the real effect of falls should be guaranteed. Moreover, it should be noted that there should be a certain time interval between the fall scene experiment and the daily activity scene experiment. The experimental results of daily activity test scenarios are shown in Table 2. In the daily activity test results, there are false positives in the experimental scenes of standing to squat, walking upstairs, and walking downstairs, which indicates that there is a certain false alarm rate in daily activities with a slight impact on the ground.

Among them, the fall test scenario experimental results are shown in Table 3. In the fall experiment test results, there were some missing reports in the forward and backward falls, but no missing reports in the fall to both sides of the body. This shows that in the process of simulated falls, the human body has certain protective actions in the process of forward and backward falls due to its self-protection consciousness, so as to reduce the violent impact with the ground.

From the above two groups of test results, we can see that the false alarm rate and false negative rate of the system are relatively low, which are 1.3% and 1.5% respectively. At present, there are no standard evaluation criteria to evaluate the fall detection system, but the sensitivity and specificity

of the fall detection system are generally used to judge the excellence of the fall detection system. Among them, the sensitivity is defined by the proportion of the number of falls detected in the total number of falls; the specificity is defined according to the proportion of the number of falls not detected in the total number of non-fall activities. In the test results of the system, the corresponding two indicators are the correct rate of the two groups of test results, which are 98.7% and 98.5% respectively.

V. CONCLUSION

With the rapid increase of the elderly population, health monitoring of the elderly has become a hot topic of social concern. With the growth of age, the muscle, bone, and other functions of the elderly begin to decline naturally, which leads to the rapid decline of balance ability, activity ability, and strain ability. Therefore, in this study, to solve the elderly health care issues, a fall detection system for the elderly wearable sensor is designed and implemented, combined with electronic and communication technology. To a large extent, it can solve the problem of the empty nest elderly living alone, so that the elderly go out alone no longer have great psychological pressure, and the children and family members of the elderly also reduce the psychological burden.

This article studies the wearable sensor network and related technologies. The concept of a wearable sensor network and its application background is summarized. The most basic attitude representation methods and their mutual conversion methods, and the basic theories of heterogeneous sensor data fusion are combed, and the process, functional model, architecture, and main methods are discussed in detail. Proposes a heterogeneous sensor data fusion algorithm based on wearable wireless body area network technology, the data fusion processing is based on the Kalman filter algorithm, which can reduce the noise interference and improve the stability of the system. Constructs a high-precision and stable wearable elderly activities of daily living (ADLs) and falls monitoring system.

Finally, it is verified through experiments. The tri-axial acceleration sensor, tri-axial magnetic sensor, and tri-axial angular velocity sensor are selected to monitor the activities of the elderly, use Bluetooth to transmit the data collected by heterogeneous sensors to smartphones, and communicate with service centers and users through mobile phone communication network, family members interact to form a wireless city network based on wearable technology. The experimental results indicate that the fall detection system designed and implemented in this study can well detect accidental falls in the daily activities of the elderly, the sensitivity and specificity of the fall detection system are 98.7% and 98.5% respectively.

The adaptability of the algorithm in this article on sensor nodes needs further verification. The algorithm verification environment proposed in this article is carried out on a personal computer, but in actual applications, the algorithm should be embedded in the sensor node, which can collect data in real-time, process data in real-time, and feedback the attitude information of the carrier in real-time. The algorithm can be applied to the actual environment. Evaluate the pros and cons of the algorithm well, so using the actual environment to test the algorithm is a problem that needs to be solved further.

REFERENCES

[1] C. Zhou, C. Tu, J. Tian, J. Feng, Y. Gao, and X. Ye, "A low power miniaturized monitoring system of six human physiological parameters based on wearable body sensor network," *Sensor Rev.*, vol. 35, no. 2, pp. 210–218, Mar. 2015.

[2] D. Antolín, N. Medrano, B. Calvo, and F. Pérez, "A wearable wireless sensor network for indoor smart environment monitoring in safety applications," *Sensors*, vol. 17, no. 2, p. 365, Feb. 2017.

[3] H. Zhang, J. Liu, and N. Kato, "Threshold tuning-based wearable sensor fault detection for reliable medical monitoring using Bayesian network model," *IEEE Syst. J.*, vol. 12, no. 2, pp. 1886–1896, Jun. 2018.

[4] E. Valero, A. Sivanathan, F. Bosché, and M. Abdel-Wahab, "Analysis of construction trade worker body motions using a wearable and wireless motion sensor network," *Autom. Construction*, vol. 83, pp. 48–55, Nov. 2017.

[5] T. Elfaramawy, C. L. Fall, S. Arab, M. Morissette, F. Lellouche, and B. Gosselin, "A wireless respiratory monitoring system using a wearable patch sensor network," *IEEE Sensors J.*, vol. 19, no. 2, pp. 650–657, Jan. 2019.

[6] Benlikaya R, Ege Y, Pándák, Zekine, "Can a wearable strain sensor based on a carbon nanotube network be an alternative to an isokinetic dynamometer for the measurement of knee-extensor muscle strength?" *Meas. Sci. Technol.*, vol. 28, no. 4, pp. 251–275, 2017.

[7] A. Binajjaj, "Design and implementation of a wearable gas sensor network for oil and gas industry workers," *J. Comput.*, vol. 4, pp. 300–308, Dec. 2018.

[8] D. Maity, K. Rajavel, and R. T. R. Kumar, "Polyvinyl alcohol wrapped multiwall carbon nanotube (MWCNTs) network on fabrics for wearable room temperature ethanol sensor," *Sens. Actuators B, Chem.*, vol. 261, pp. 297–306, May 2018.

[9] X. Guo, "Highly stretchable strain sensor based on SWCNTs/CB synergistic conductive network for wearable human-activity monitoring and recognition," *Smart Mater. Struct.*, vol. 26, no. 9, 2017, Art. no. 095017.

[10] H. Ghasemzadeh, "Power-aware computing in wearable sensor networks: An optimal feature selection," *IEEE Trans. Mobile Comput.*, vol. 14, no. 4, pp. 800–812, Apr. 2015.

[11] H. Lin, W. Xu, N. Guan, D. Ji, Y. Wei, and W. Yi, "Noninvasive and continuous blood pressure monitoring using wearable body sensor networks," *IEEE Intell. Syst.*, vol. 30, no. 6, pp. 38–48, Nov. 2015.

[12] L. Yu, D. Xiong, L. Guo, and J. Wang, "A remote quantitative fuglmeyer assessment framework for stroke patients based on wearable sensor networks," *Comput. Methods Programs Biomed.*, vol. 128, pp. 100–110, May 2016.

[13] H. F. Nweke, Y. W. Teh, M. A. Al-garadi, and U. R. Alo, "Deep learning algorithms for human activity recognition using mobile and wearable sensor networks: State of the art and research challenges," *Expert Syst. Appl.*, vol. 105, pp. 233–261, Sep. 2018.

[14] Y. Yao, Q. Cao, and A. V. Vasilakos, "EDAL: An energy-efficient, delay-aware, and lifetime-balancing data collection protocol for heterogeneous wireless sensor networks," *IEEE/ACM Trans. Netw.*, vol. 23, no. 3, pp. 810–823, Jun. 2015.

[15] M. Elhoseny, X. Yuan, Z. Yu, C. Mao, H. K. El-Minir, and A. M. Riad, "Balancing energy consumption in heterogeneous wireless sensor networks using genetic algorithm," *IEEE Commun. Lett.*, vol. 19, no. 12, pp. 2194–2197, Dec. 2015.

[16] F. Zhao, W. Wang, H. Chen, and Q. Zhang, "Interference alignment and game-theoretic power allocation in MIMO heterogeneous sensor networks communications," *Signal Process.*, vol. 126, pp. 173–179, Sep. 2016.

[17] M. S. Farash, M. Turkanovi, S. Kumari, and M. Hölbl, "An efficient user authentication and key agreement scheme for heterogeneous wireless sensor network tailored for the Internet of Things environment," *Ad Hoc Netw.*, vol. 36, pp. 152–176, Jan. 2016.

[18] Z. Hong, R. Wang, and X. Li, "A clustering-tree topology control based on the energy forecast for heterogeneous wireless sensor networks," *IEEE/CAA J. Automatica Sinica*, vol. 3, no. 1, pp. 70–79, Dec. 2016.
[19] S. M. Jameii, K. Faez, and M. Dehghan, "AMOF: Adaptive multi-objective optimization framework for coverage and topology control in heterogeneous wireless sensor networks," *Telecommun. Syst.*, vol. 61, no. 3, pp. 515–530, Mar. 2016.
[20] J. Medina, L. Martínez, and M. Espinilla, "Subscribing to fuzzy temporal aggregation of heterogeneous sensor streams in real-time distributed environments," *Int. J. Commun. Syst.*, vol. 30, no. 5, p. e3238, Mar. 2017.
[21] S. Zhu, Y. Guo, J. Chen, D. Li, and L. Cheng, "Integrating optimal heterogeneous sensor deployment and operation strategies for dynamic origin-destination demand estimation," *Sensors*, vol. 17, no. 8, p. 1767, Aug. 2017.
[22] H. Bagci, I. Korpeoglu, and A. Yazici, "A distributed fault-tolerant topology control algorithm for heterogeneous wireless sensor networks," *IEEE Trans. Parallel Distrib. Syst.*, vol. 26, no. 4, pp. 914–923, Apr. 2015.
[23] J. Tian, T. Yan, and G. Wang, "A network coding based energy efficient data backup in survivability-heterogeneous sensor networks," *IEEE Trans. Mobile Comput.*, vol. 14, no. 10, pp. 1992–2006, Oct. 2015.
[24] J. Szurley, A. Bertrand, and M. Moonen, "Distributed adaptive node-specific signal estimation in heterogeneous and mixed-topology wireless sensor networks," *Signal Process.*, vol. 117, pp. 44–60, Dec. 2015.
[25] J. Guo and H. Jafarkhani, "Sensor deployment with limited communication range in homogeneous and heterogeneous wireless sensor networks," *IEEE Trans. Wireless Commun.*, vol. 15, no. 10, pp. 6771–6784, Oct. 2016.
[26] Y. Chen, F. Liu, S. Mei, and J. Ma, "A robust WLAV state estimation using optimal transformations," *IEEE Trans. Power Syst.*, vol. 30, no. 4, pp. 2190–2191, Jul. 2015.
[27] Y. Chen, J. Ma, P. Zhang, F. Liu, and S. Mei, "Robust state estimator based on maximum exponential absolute value," *IEEE Trans. Smart Grid*, vol. 8, no. 4, pp. 1537–1544, Jul. 2017.
[28] Y. Chen, Y. Yao, and Y. Zhang, "A robust state estimation method based on SOCP for integrated electricity-heat system," *IEEE Trans. Smart Grid*, vol. 12, no. 1, pp. 810–820, Jan. 2021, doi: 10.1109/TSG.2020.3022563.
[29] P. Kim, *Kalman Filter for Beginners: With MATLAB Examples*. Seoul, South Korea: National Rehabilitation Research Institute of Korea, 2011.
[30] Tariqul I, Md. Saiful, Md. Shajid, "Comparison of complementary and Kalman filter based data fusion for attitude heading reference system," *AIP Conf. Proc.*, vol. 1919, Feb. 2017, Art. no. 020002.
[31] J. Barcel, "Robustness and computational efficiency of Kalman filter estimator of time-dependent origin-destination matrices exploiting ICT traffic measurements," *Transp. Res. Rec.*, vol. 12, no. 4, pp. 31–39, 2013.
[32] D. Willner, C. Chang, and K. Dunn, "Kalman filter configurations for multiple radar systems," Massachusetts Inst. Technol., Cambridge, MA, USA, Tech. Rep. TN-1976-21, 2012.

DAOHUA PAN was born in Harbin, Heilongjiang, China, in 1981. She received the bachelor's degree from the Heilongjiang University of Science and Technology, China. She is currently pursuing the degree with the School of Computer Science and Technology, Harbin Institute of Technology. She is currently with the Department of Electronic and Information Engineering, Heilongjiang Vocational College for Nationalities. Her research interests include AI, pattern recognition, pervasive computing, and wearable computer and system evaluation theory and technology.

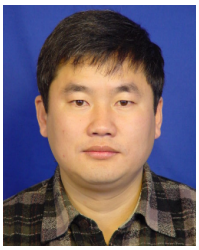

HONGWEI LIU received the Ph.D. degree in computer science and technology from the Harbin Institute of Technology. He is currently a Professor with the School of Computer Science and Technology, Harbin Institute of Technology. He is a member of the Expert Committee for Information Field, National High-tech Research and Development Program of China (863 Program). His research interests include parallel computing and architecture, fault tolerant computer, computer system architecture evaluation theory and technology, availability optimization, and resource scheduling in cloud computing.

DONGMING QU received bachelor's degree in computer science and technology from Harbin Engineering University, in 2003. He is currently a Technical Engineer with the Department of Financial Technology, China Construction Bank, Heilongjiang. His research interests include the theory and technology of smart payment and Internet finance.